Molecular Cell
Article

Cell-Type-Specific Control of Enhancer Activity by H3K9 Trimethylation

Yina Zhu,[1] Dominic van Essen,[1,*] and Simona Saccani[1,*]
[1]Department of Cellular and Molecular Immunology, Max Planck Institute for Immunobiology and Epigenetics, Stübeweg 51, 79108 Freiburg, Germany
*Correspondence: vanessen@immunbio.mpg.de (D.v.E.), saccani@immunbio.mpg.de (S.S.)
DOI 10.1016/j.molcel.2012.05.011

SUMMARY

Cell-type-specific control of gene expression is critical for the development of multicellular organisms. To investigate the mechanisms which underlie this, we have studied the regulation of the model genes *Mdc* and *Il12b*, whose stimulus-induced expression is tightly restricted to specific cells of the immune system. Surprisingly, we find that neither the promoter nor the enhancer sequences of these genes are sufficient to direct this cell-type specificity. Instead, the activities of upstream enhancers are repressed in nonexpressing cells by high levels of trimethylated H3K9 in their flanking regions. Genome-wide analysis indicates that this manner of regulation is shared by numerous enhancers of cell-type-specific genes. In dendritic cells and macrophages, the stimulus-induced demethylase Jmjd2d controls H3K9me3 levels at these regions, and is thereby required for *Mdc* and *Il12b* transcription. By experimentally assaying multiple enhancers in a variety of cell types, we show that regulation by H3K9me3 is a widely used mechanism which imparts specificity to the activities of otherwise broadly functional enhancers.

INTRODUCTION

The precise regulation of gene expression underlies the ability of all living organisms to respond to stimuli and is essential for metazoan development and differentiation. In mammals, the stimulus-induced expression of inflammatory genes represents a good model system to study the mechanisms which control the specificity of gene expression. Inflammation is triggered by the rapid and specific activation of multiple genes by cells of the innate immune system, in response to tissue injury and infection (Smale, 2010). Activation of most inflammatory genes is driven by the binding to proximal promoter elements of stimulus-inducible transcription factors, exemplified by NF-κB. NF-κB is an evolutionarily conserved family of transcription factors, which are active in most metazoan cell types (Hoffmann and Baltimore, 2006). However, many of its target genes display highly restricted patterns of expression (Hoffmann and Baltimore, 2006; Natoli and De Santa, 2006; Sen and Smale, 2010; Smale, 2010), indicating that additional processes control their cell-type specificity.

RESULTS

Expression of the *Mdc* and *Il12b* Genes, but Not the Function of Their Promoter or Enhancer Sequences, Is Strictly Cell-Type Specific

Exposure to inflammatory stimuli such as LPS elicits strong expression of the NF-κB-dependent *Mdc* and *Il12b* genes by myeloid cells such as dendritic cells (DCs; Figure 1A). However, these genes are not expressed at all in stimulated 3T3 fibroblasts, even using much higher amounts of LPS or using TNF-α (a more potent NF-κB-inducing stimulus in this cell type; Figure 1A and see Figure S1B online).

To separate the contributions of *cis*-acting motifs in the promoters or enhancers of these genes (see Figure S1A) from the possible regulatory effects of their native chromatin context, we began by cloning the 1 kb sequences immediately upstream of the transcriptional start sites of each into a plasmid vector, to drive expression of a green fluorescent protein (GFP) reporter gene. We then assayed their activities after transfection into either a myeloid macrophage cell line or into fibroblasts. Using this system, we could readily detect the cell-type-specific activity of a previously characterized control promoter derived from the human *SR1* gene, which drives GFP expression only in macrophages (Figure 1B; Horvai et al., 1995). The promoter regions of *Mdc* and *Il12b* recapitulated the NF-κB responsiveness of their endogenous genes (as described; Ghadially et al., 2005; Murphy et al., 1995; Figure 1B). However, in contrast to the cell-type-specific expression of the endogenous *Mdc* and *Il12b* genes, their promoter regions were able to drive NF-κB-dependent GFP expression when transfected both into macrophages and into fibroblasts (Figure 1B). Moreover, their promoter regions exhibited significant basal activity in both cell types when combined with enhancer elements on the same plasmid (Figure S1C). Thus, the primary sequences of the *Mdc* and *Il12b* proximal promoter regions are not sufficient to direct their cell-type-specific gene expression.

To identify distal *cis*-regulatory elements at the *Il12b* and *Mdc* loci, we began by using chromatin IP (ChIP) to measure levels of monomethylated H3K4, since peaks of H3K4me1 have been shown to correlate with promoter/enhancer elements that are functional in a given cell type (Heintzman et al., 2009). As expected, we found that the *Mdc* and *Il12b* promoters are marked by local H3K4me1 in DCs (Figures 1D and 1E). In addition, this

analysis revealed several distal peaks of H3K4me1, suggesting the possible locations of enhancers. In fibroblasts, H3K4me1 was absent from the promoters of both genes, and from a subset of additional locations at the *Il12b* locus. Notably, however, regions upstream of both genes contained putative enhancers which still remained strongly associated with H3K4me1 peaks in fibroblasts (Figures 1D and 1E), despite their inability in this cell type to activate transcription from the associated promoters.

The upstream peak at the *Il12b* locus in fibroblasts corresponds to an enhancer which was previously functionally characterized in macrophages (Zhou et al., 2007; see also Figure S1D). We screened sequences up to 15 kb upstream of the *Mdc* transcriptional start site using a transfection-based reporter assay, and found that the H3K4me1 peak at −10 kb also coincides with a functional enhancer element (Figure S1D). To investigate whether either of these enhancers could exhibit cell-type-specific function, we examined their abilities to enhance GFP expression driven from a minimal promoter on a reporter plasmid when transfected into either macrophages or fibroblasts. With this assay, we could measure the cell-type-specific function of numerous control enhancers (such as that of *Il1b*; Figure 1C and Figure S1E). However, although the endogenous *Mdc* and *Il12b* enhancers fail to drive expression of their target genes in fibroblasts (Figure 1A), these enhancer sequences were functional on episomal reporter plasmids when transfected into both cell types (Figure 1C and Figure S1D). We also obtained the same results by pairing each enhancer with its own proximal promoter, excluding the possibility that cell-type-specific activity might result from differences in compatibility with these particular promoters (Figure S1F).

Although the episomal assay is widely used to measure cell-type-specific enhancer function (Bulger and Groudine, 2011; Ghisletti et al., 2010; Heintzman and Ren, 2009), and activity in this assay unambiguously reveals the functionality of a particular sequence and the availability of specific activating transcription factors in a given cell type, it differs from the natural situation in which enhancers (and their target promoters) are embedded within genomic chromatin. To examine the function of the *Mdc* and *Il12b* enhancers in this setting, we used a self-inactivating retroviral vector (lacking viral enhancer elements) to integrate each enhancer, together with a minimal promoter-GFP reporter, into multiple genomic locations. Again, we found that both enhancers could still drive stable GFP expression after transduction into either macrophages or fibroblasts (Figure 1C), indicating that they are also broadly functional in the context of chromatin.

It is important to make a distinction whether, in a given cell type, promoter/enhancer sequences are *functional*, by which we refer to their inherent ability to drive gene expression when assayed in isolation (such as on a reporter plasmid), or whether endogenous promoter/enhancers are *active*, by which we denote their ability to drive gene expression when both are in their native genomic and chromatin context. The function of a promoter or enhancer is usually considered to be determined by the availability and binding of particular combinations of activating and/or repressing transcription factors (Borok et al., 2010; Levine and Tjian, 2003; Visel et al., 2009). However, the above experiments show that the *Mdc* and *Il12b* promoters (Figure 1B) and enhancers (Figure 1C) are both functional in fibroblasts, and yet the endogenous genes are not expressed, suggesting that their cell-type-specific genomic environment provides an additional level of regulation.

To investigate this further, we used ChIP to survey the chromatin landscape of the endogenous *Mdc* and *Il12b* loci, both in DCs, which express these genes upon stimulation, and in fibroblasts, which do not (Figure 1A). We began by examining H3K27Ac (another chromatin mark correlating with enhancer function; Creyghton et al., 2010; Rada-Iglesias et al., 2011) and acetylated H4 (which is generally associated with active transcription): in DCs, both of these marks were present at the *Mdc* and *Il12b* enhancers before stimulation, and they were also robustly induced at the promoters of both genes upon stimulation (Figures S1G–S1J). In 3T3 fibroblasts, although neither mark was detected at the inactive promoters of these genes, both were strongly present at their enhancer regions, before and after stimulation (Figures S1G–S1J).

We also investigated the abilities of selected sequence-specific transcription factors to bind to these enhancers in both cell types. The NF-κB subunit c-Rel is known to regulate the expression of both *Mdc* and *Il12b* (Sanjabi et al., 2000; van Essen et al., 2010), and the transcription factor CEBP/β has previously been described to bind to the *Il12b* promoter and enhancer (Plevy et al., 1997; Zhou et al., 2007). In DCs, we could detect inducible binding of c-Rel to the promoters and upstream enhancers of both genes, and of CEBP/β to the *Il12b* enhancer (Figures S1K and S1L). Strikingly, although c-Rel could no longer be found at the *Mdc* or *Il12b* promoters in 3T3 fibroblasts, both transcription factors bound to the upstream enhancer regions, at levels comparable to those seen in unstimulated DCs (Figures S1K and S1L).

Thus, the presence of histone modifications correlating with active transcription, together with the binding of specific transcription factors, supports the results of our reporter assays above and suggests that the endogenous *Mdc* and *Il12b* enhancers are functional in 3T3 fibroblasts. Despite this, they are unable to activate gene expression upon cellular stimulation, implying that their activities could be subject to negative regulation in this cell type.

H3K9me3-Rich Regions Flank Many Enhancers of Inactive Genes in Nonexpressing Cell Types

H3K9 trimethylation is generally associated with transcriptional silencing in heterochromatin (Hublitz et al., 2009; Kouzarides, 2007), and when we examined the behavior of this modification at the *Mdc* and *Il12b* loci, we observed a striking difference between DCs and 3T3 fibroblasts upon stimulation. Before stimulation, in both cell types, only low levels of H3K9me3 were present at the promoters of these genes, but upstream genomic locations spanning the enhancers of both *Mdc* and *Il12b* contained regions of higher-level H3K9me3. Although embedded between these regions, the enhancers themselves were spared from the highest levels of H3K9me3, which were instead located at around 3–6 kb on either side (Figures 2A and 2B). After stimulation of DCs, H3K9me3 levels surrounding the enhancer regions either remained unchanged or were locally reduced (Figures 2A and 2B and Figure S2B), accompanying the

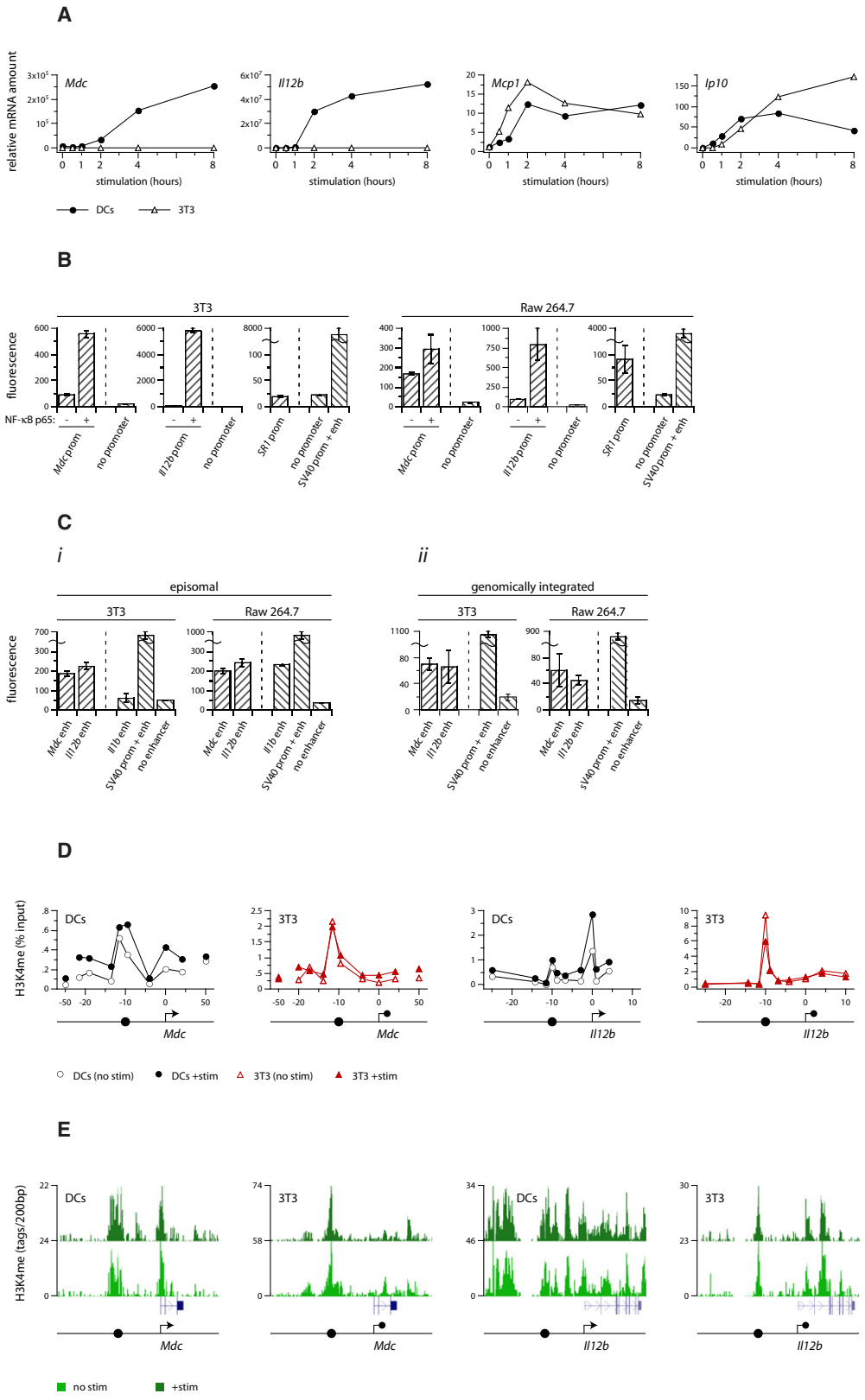
A
relative mRNA amount
Mdc
Il12b
Mcp1
Ip10
stimulation (hours)
DCs
3T3
B
3T3
Raw 264.7
fluorescence
NF-κB p65:
Mdc prom
no promoter
Il12b prom
SP1 prom
SV40 prom + enh
C
i
ii
episomal
genomically integrated
Mdc enh
Il12b enh
Il1b enh
no enhancer
D
H3K4me (% input)
DCs
3T3
Mdc
Il12b
DCs (no stim)
DCs +stim
3T3 (no stim)
3T3 +stim
E
H3K4me (tags/200bp)
no stim
+stim

induction of gene expression and the acquisition of promoter chromatin marks associated with transcriptional activation (Figure 1A and Figures S1G–S1J). In contrast, stimulation of 3T3 fibroblasts induced a further increase in H3K9me3 which decorated the entire *Mdc* and *Il12b* gene loci, with the peak amounts again flanking, but largely excluding, the two enhancers (Figures 2A and 2B). These high and induced levels of H3K9 trimethylation were a particular feature of the nonexpressed *Mdc* and *Il12b* gene loci; at several control genes which are expressed in stimulated fibroblasts, H3K9me3 levels were low and remained low after stimulation (Figures S1B, S2A, and S2D). We observed high levels of H3K9 trimethylation in 3T3 fibroblasts treated with two independent stimuli (TNF-α and LPS; Figure S2C), both of which are unable to induce *Mdc* or *Il12b* expression in this cell type but which do trigger expression of other inflammatory NF-κB target genes (Figure S1B).

Thus, the high levels of H3K9me3 surrounding the *Mdc* and *Il12b* enhancers in fibroblasts correlate with the failure of these functional enhancers to activate transcription at their target genes in this cell type upon stimulation. To extend these observations to other enhancers throughout the genome, we first used our H3K4me1 ChIP data to identify a set of around 80,000 peaks, corresponding to the locations of putative enhancers. We then interrogated these for the surrounding distribution of H3K9me3 in DCs and fibroblasts, before and after stimulation. Similarly to what we had observed at the *Mdc* and *Il12b* loci, we found that H3K9me3 is present on average at only low-to-moderate levels near promoters (Figure 2C), and the proximal promoter regions themselves tend to be particularly depleted of H3K9me3. The frequency of H3K9 trimethylation increases with distance upstream of promoters, so that in the vicinity of the adjacent enhancer regions it is typically present at an elevated level (Figure 2C). As with promoters, enhancers themselves specifically exclude the highest amounts of H3K9me3, which is depleted on either side of enhancers up to distances of around 3 kb. This pattern was observed with both fibroblasts and DCs, and also using publically available data sets derived from several human cell types (Figure S2F), and using distinct sets of enhancers independently predicted in other cell types (e.g., HeLa cells, Figures S2E and S2F; K652 cells, data not shown; Heintzman et al., 2009). For comparison, we also examined the genome-wide distributions of other histone modifications associated with transcriptional repression: while several of these show a characteristic pattern of enrichment or depletion at promoter regions (as previously described; Barski et al., 2007), only depletion of H3K9me3 showed a pronounced correlation with the locations of predicted enhancers, strongly suggestive of a link with enhancer function in multiple cell types (Figure S2E).

Guided by our observations of the H3K9me3 levels surrounding the model enhancers of the *Mdc* and *Il12b* genes (Figures 2A and 2B), and on the genome-wide distribution of this modification around other predicted enhancers (Figure 2C), we examined total H3K9me3 levels flanking each enhancer at distances from 3 to 10 kb away. The levels of H3K9me3 surrounding predicted enhancers negatively correlate with the magnitudes of histone modifications associated with transcriptional activation at the enhancers themselves (Figure 2D), suggesting that enhancers flanked by high-level H3K9me3 are indeed inactive.

To investigate this, we compared the levels of H3K9me3 flanking enhancers with the expression levels of their adjacent genes in DCs and fibroblasts (which we determined using microarray analysis). Enhancers with high levels of flanking H3K9me3 are selectively enriched adjacent to nontranscribed genes (Figure 2E and Figure S2F), analogous to the situation which has been described for promoters (Barski et al., 2007). Moreover, cell-type-specific changes in gene expression are accompanied by changes in the levels of H3K9me3 around adjacent enhancers: that is, when inactive genes associated with enhancers flanked by high-level H3K9me3 are active in a different cell type, the levels of H3K9me3 around these enhancers are also strongly reduced (Figure 2E and Figure S2G). Although high levels of H3K9me3 at regions flanking enhancers and at promoters both correlate with gene inactivity, they do not always occur together, indicating that they can be regulated independently (Figure S2H). Hence, even when considering only promoters bearing low H3K9me3, the strong correlation between promoter inactivity and the H3K9 trimethylation surrounding their adjacent enhancers still holds true. In addition, gene inactivity correlates with high levels of H3K9me3 around adjacent enhancers even when these are separated from promoters by large intervening distances (>100 kb; Figure S2H).

To investigate whether H3K9me3 levels flanking enhancers may regulate dynamic changes in gene expression, we focused on the behavior of enhancers adjacent to genes which are stimulus inducible in DCs. In unstimulated fibroblasts, prior to the induction of gene expression, these enhancers tend to be flanked by predominantly low levels of H3K9me3 (Figure 2F). Upon stimulation, enhancers adjacent to genes whose expression is also induced in fibroblasts retained these low levels of flanking H3K9me3. In contrast, at genes which are inducible in DCs but inactive in fibroblasts, around 35% of the adjacent

Figure 1. Expression of the *Mdc* and *Il12b* Genes, but Not the Function of Their Promoter or Enhancer Sequences, Is Strictly Cell-Type Specific

(A) Expression of *Mdc*, *Il12b*, *Mcp1*, and *Ip10* mRNA in DCs stimulated with LPS, and in 3T3 fibroblasts stimulated with TNF-α, relative to levels in unstimulated 3T3s.

(B) Fluorescence intensities of 3T3 fibroblasts and Raw264.7 macrophages after cotransfection with GFP reporter vectors containing the indicated promoter sequences, together with an NF-κB p65 expression vector (similar results were also obtained using NF-κB c-Rel [data not shown]).

(C) Fluorescence intensities of cells containing minimal promoter-GFP reporter vectors carrying the indicated enhancer sequences; (Ci) transient transfection with episomal plasmid vectors, (Cii) stable transduction with self-inactivating retroviral vectors. Control transfections are shown to the right of the dotted lines. Error bars indicate SEMs of replicate transfections.

(D and E) H3K4me1 levels at the *Mdc* and *Il12b* loci in DCs stimulated for 2 hr with LPS, and in 3T3s stimulated with TNF-α, measured by ChIP followed by quantitative PCR (D) or high-throughput sequencing (E). The positions of promoters and the studied enhancers for each gene are shown schematically below each panel. The results presented in (A)–(D) are representative of three to ten experiments. Statistical analysis and related experiments are described in Figure S1.

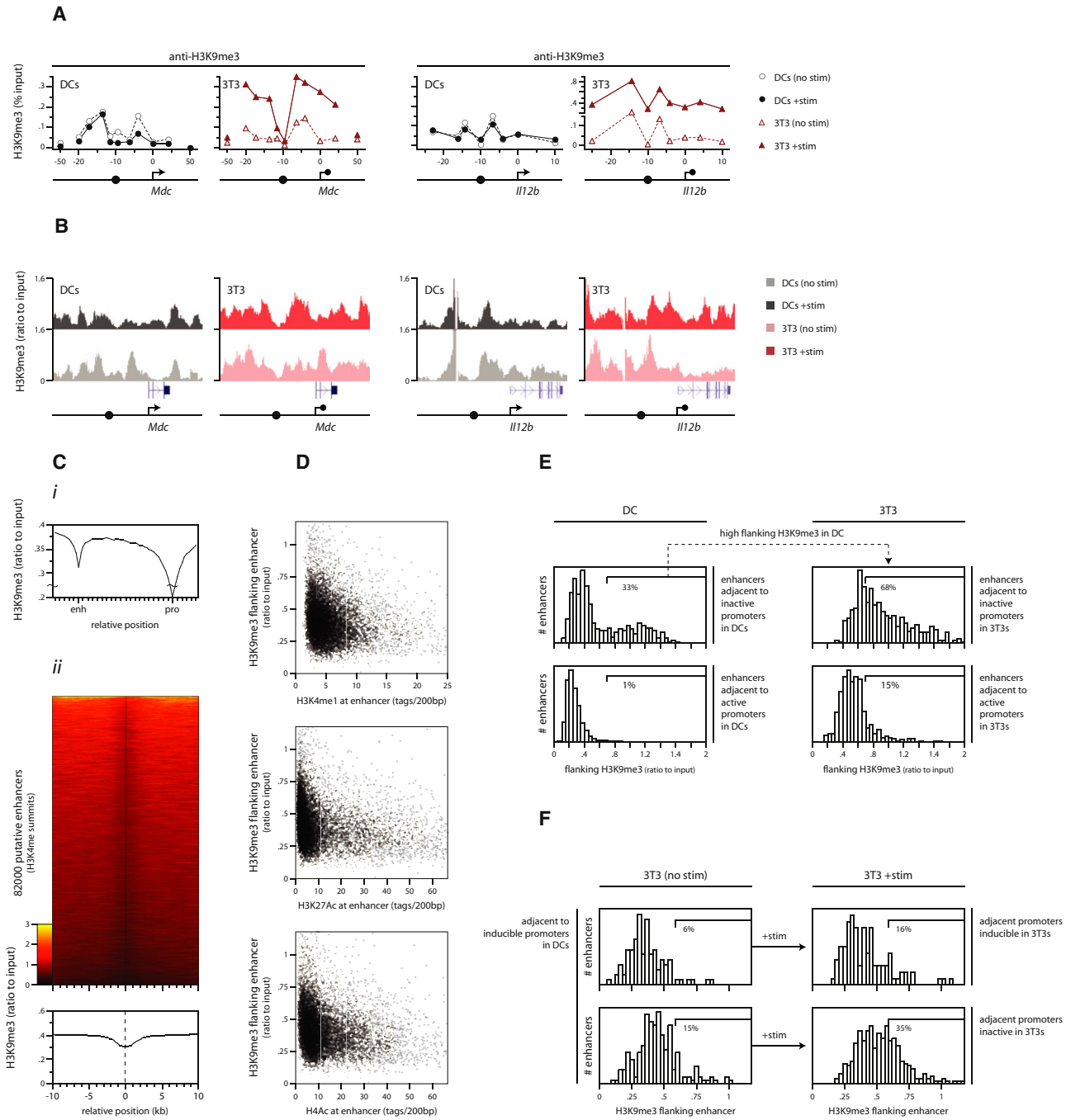

Figure 2. H3K9me3-Rich Regions Flank Many Enhancers of Inactive Genes in Nonexpressing Cell Types

(A and B) H3K9me3 levels at the *Mdc* and *Il12b* loci in DCs and 3T3 fibroblasts, measured as in Figures 1D and 1E.

(C) Levels of H3K9me3 in 3T3 fibroblasts (Ci) between predicted enhancers and their nearest promoters, and (Cii) surrounding predicted enhancers. Line graphs indicate the average levels for all enhancers; heatmap in (Cii) depicts the levels surrounding each individual enhancer.

(D) H3K4me1, H3K27Ac, and H4Ac levels at predicted enhancers (±2 kb), versus the level of flanking H3K9me3 (−10 to −3, and 3–10 kb). Each dot represents the levels at an individual enhancer.

(E) (Left) Distributions of flanking H3K9me3 levels in unstimulated DCs, around predicted enhancers which are adjacent to inactive (top) or active (bottom) promoters in this cell type. (Right) Distributions of flanking H3K9me3 levels in unstimulated 3T3 fibroblasts, around only those enhancers which were flanked by high levels of H3K9me3 in DCs.

(F) Distributions of flanking H3K9me3 levels in 3T3s, around predicted enhancers which are adjacent to the promoters of genes which are stimulus inducible in DCs, and either inducible (top) or nonexpressed (bottom) in 3T3 fibroblasts. (Left) Unstimulated 3T3s; (right) 3T3s stimulated for 2 hr with TNF-α. The results presented in (A) are representative of five experiments. Statistical analysis and related experiments are described in Figure S2.

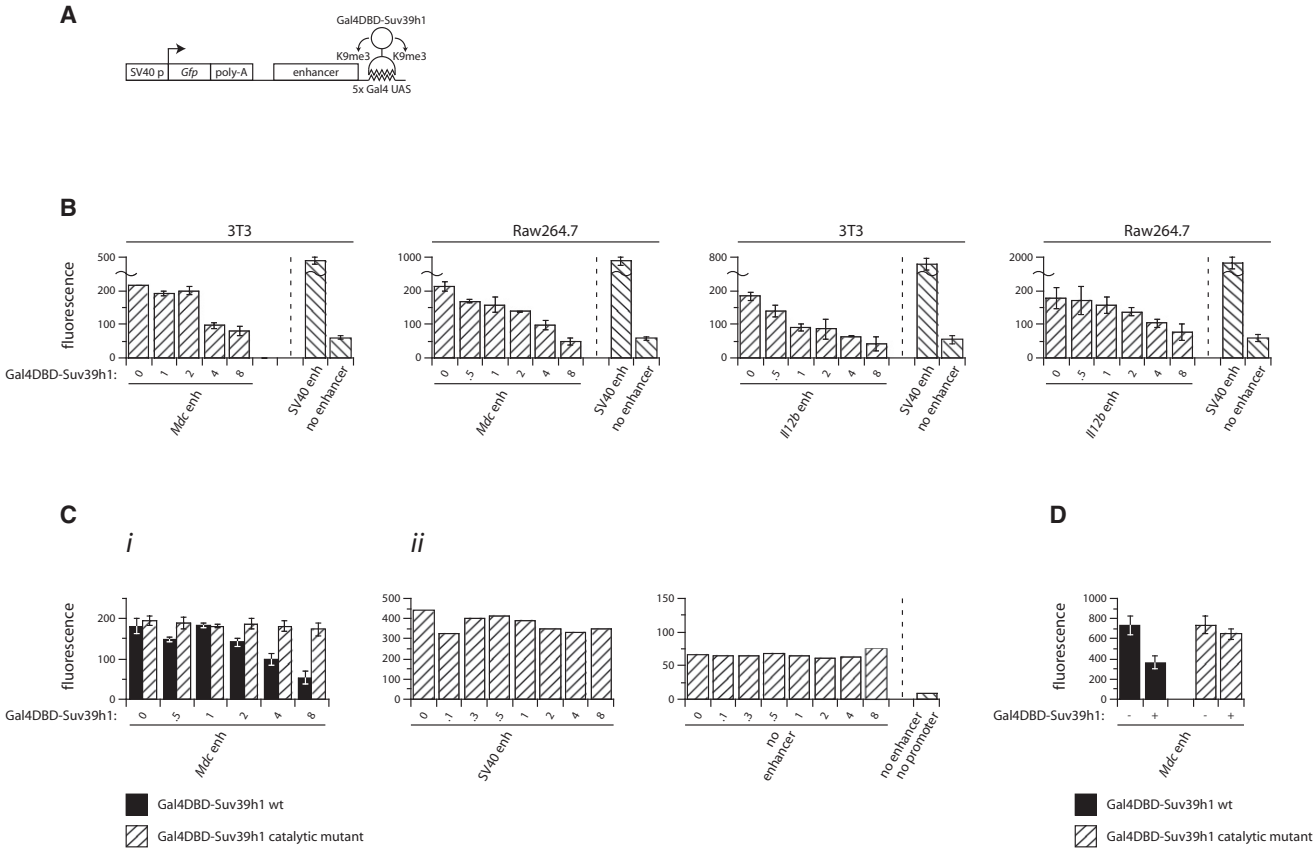

Figure 3. The Activities of the *Mdc* and *Il12b* Enhancers Are Repressed by H3K9 Trimethylation

(A) Schematic diagram of the episomal reporter plasmid used.

(B and C) Fluorescence intensities of 3T3 fibroblasts and Raw264.7 macrophages cotransfected with the GFP reporter vector together with increasing relative amounts of a Gal4DBD-Suv39h1 expression vector. (C) The repressive effect of Gal4DBD-Suv39h1 was (Ci) compared with that of its catalytic mutant or (Cii) assayed using reporter vectors containing either the strong SV40 enhancer, or without any enhancer. Control transfections are shown to the right of the dotted lines.

(D) Repression of genomically integrated reporter vectors, by transient transfection of the Gal4DBD-Suv39h1 expression vector, or its catalytic mutant. Error bars indicate SEMs of independent transfections. The results presented here are representative of two to ten experiments. Statistical analysis and related experiments are described in Figure S3.

enhancers inducibly acquired higher levels of H3K9me3 in their flanking regions (Figure 2F), reminiscent of the situation observed at the *Mdc* and *Il12b* loci (Figures 2A and 2B).

Together, these results reveal that the H3K9me3 levels flanking a subset of enhancers are predictive of the cell-type-specific or stimulus-inducible expression of their putative target genes.

The Activities of the *Mdc* and *Il12b* Enhancers Are Repressed by H3K9 Trimethylation

It has been shown that H3K9 trimethylation can negatively regulate promoter activity (Snowden et al., 2002). However, despite its widespread distribution in intergenic regions (Hawkins et al., 2010; Mikkelsen et al., 2007; Figures 2A–2C and Figures S2D and S2F), its impact on the activity of enhancers and other distal regulatory elements has been little studied. The above experiments suggested that the hypermethylation of H3K9 induced around enhancers might be functionally involved in repressing their activites in nonexpressing cellular contexts. Alternatively, though, this might simply be an indirect reflection of the activity of some unconnected repressive mechanism(s), or it might even be a downstream consequence of enhancer inactivity. To discriminate between these possibilities, we examined the effect of artificially targeting H3K9 trimethylation to functional enhancers, after they have been removed from the influence of any regulation conferred by their natural chromosomal context.

We introduced a Gal4-binding motif adjacent to either the *Mdc* or *Il12b* enhancer sequences and distal to the promoter in our episomal reporter plasmid, and cotransfected this into cells along with a plasmid driving expression of the H3K9 methyltransferase Suv39h1, fused to the DNA-binding domain of yeast Gal4 (Figure 3A). The activity of Gal4-Suv39h1 resulted in locally increased H3K9 trimethyation around the enhancer region, and not at the reporter gene promoter, located at a distance of around 3 kb on the same plasmid (Figure S3A). Expression of Gal4-Suv39h1 also resulted in a dose-dependent repression of *Mdc* and *Il12b* enhancer activity, both in 3T3 fibroblasts and

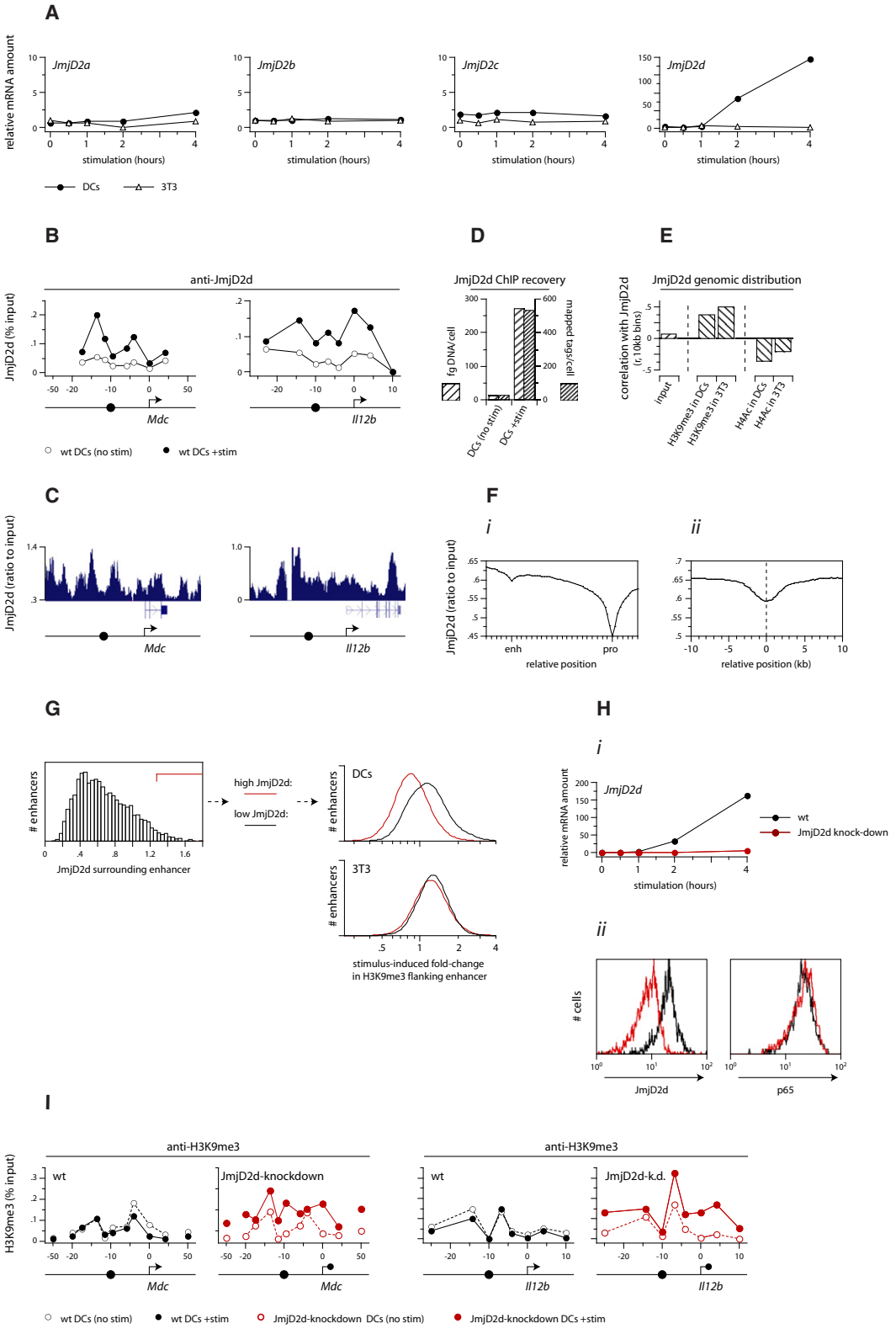

Figure 4. JmjD2d Is a Cell-Type-Specific Demethylase which Controls H3K9me3 Levels around the *Mdc* and *Il12b* Enhancers

(A) Expression *of JmjD2a-d* mRNA in DCs stimulated with LPS, and in 3T3 fibroblasts stimulated with TNF-α, relative to levels in unstimulated 3T3s.

(B and C) Recruitment of JmjD2d protein to the *Mdc* and *Il12b* loci in DCs stimulated for 2 hr with LPS, measured as in Figures 1D and 1E.

in macrophages, to the extent that the contribution of enhancer activity to reporter expression was almost completely eliminated (Figure 3B). This repression was directly dependent on methyltransferase activity, since expression of a mutant form of Gal4-Suv39h1 with no catalytic activity was unable to repress the *Mdc* enhancer (Figure 3C and Figure S3B). Basal promoter activity without any enhancer was unaffected by Gal4-Suv39h1 (Figure 3C), further indicating that its repressive effect in this setup is mediated through regulation of enhancer activity, and not through a nonspecific inhibition of transcription from the transfected plasmid. In agreement with this, Gal4-Suv39h1 was unable (or insufficient) to repress the activity of the very strong SV40 enhancer when present on an otherwise identical plasmid.

Targeted H3K9 methylation was also able to repress enhancer activity in a genomically integrated reporter (Figure 3D), although to a lesser extent than the complete shutoff observed in the episomal assay.

Thus, these data together indicate that enhancer activity can be directly repressed by a mechanism dependent on H3K9 trimethylation.

Jmjd2d Is a Cell-Type-Specific Demethylase which Controls H3K9me3 Levels around the *Mdc* and *Il12b* Enhancers

These results illustrate that cell-type-specific differences in local levels of H3K9me3 are sufficient to explain differences in the activities of otherwise broadly functional enhancers, such as those of *Mdc* and *Il12b*. This implies that there should exist cell-type-specific mechanisms which control the H3K9me3 levels around such enhancers, and that experimental disruption of these should interfere with target gene expression. To test this, we therefore sought to understand how the induction of H3K9me3 could be regulated in a cell-type-specific fashion at the *Mdc* and *Il12b* loci.

We noted that within the regions flanking the *Mdc* and *Il12b* enhancers which bear higher levels of H3K9me3 there are several discrete locations which undergo a gradual reduction in H3K9 trimethylation in stimulated DCs (Figure S2B). This hinted that a histone demethylase activity may contribute to the control of local H3K9me3 levels at these loci. We investigated the expression levels of the JmjD2 family of H3K9me3 demethylases (Nottke et al., 2009) upon stimulation of DCs, and compared them with their levels in stimulated 3T3 fibroblasts. Expression levels of *JmjD2a*, *JmjD2b* and *JmjD2c* mRNAs were not induced by stimulation and were similar in DCs and fibroblasts. Strikingly, however, *JmjD2d* mRNA was induced in DCs by both LPS and (to a lesser extent) TNF-α stimulation, to levels which exceeded those found in fibroblasts by up to 80-fold (Figure 4A and Figure S4A). We examined *JmjD2d* mRNA levels in a panel of mouse organs and found that the highest expression levels were prominent in the brain and hematopoietic system (spleen, lymph nodes, and bone marrow; Figure S4A). This expression pattern of *JmjD2d*, together with its upregulation in DCs in response to LPS, implicated it as a potential regulator of H3K9me3 levels in myeloid cells.

We generated monoclonal antibodies (Figure S5) specific for the C-terminal region of JmjD2d (which does not share any homology with the other JmjD2 family members), and specific for its JmjN domain (which is conserved in all JmjD2 family members), and used these to examine the binding profile of JmjD2d protein in stimulated DCs by ChIP. We found JmjD2d associated with the *Mdc* and *Il12b* loci, with a profile encompassing the regions flanking the enhancers, but also spreading further to upstream and downstream locations (Figures 4B and 4C). The recovery was significantly reduced in *JmjD2d* knockdown DCs (see later; Figure S4B) and in resting DCs without stimulation (Figure 4B and Figure S4B). We also detected a similar profile using antibodies recognizing a tagged form of JmjD2d expressed from a retroviral vector in transduced DCs (Figure S4C), and using our antibody specific for the JmjN domain (Figures S4D and S4F). JmjD2d did not associate with several other tested genomic locations, including other genes whose expression is induced in stimulated DCs (Figure S4E), indicating that it must be governed by specific targeting mechanisms.

To investigate this further, we surveyed the binding of JmjD2d across the genome, using ChIP data generated from unstimulated and stimulated DCs. Overall, although the magnitude of binding was increased by around 20-fold upon stimulation (measured by ChIP recovery; Figure 4D), the profiles of JmjD2d binding were highly similar both before and after stimulation. JmjD2d binding strongly correlates with the distribution of its substrate, H3K9me3 (recalling the described match between the binding pattern of histone deacetylase enzymes and acetylated histones; Wang et al., 2009), such that both were enriched in transcriptionally inactive, gene-poor genomic domains. However, the association with H3K9me3 was also clearly apparent in gene-rich genomic regions (Figure 4E), and JmjD2d showed an average binding profile around promoters and enhancers which resembled the distribution of H3K9me3 (Figure 4F and Figure S4G).

(D) Quantitation of total recovered DNA and mapped sequence reads, after ChIP for JmjD2d from unstimulated DCs, or DCs stimulated for 2 hr with LPS.
(E) Correlation of JmjD2d binding in stimulated DCs, in 10 kb intervals within transcriptionally active genomic regions (see the Experimental Procedures), with H3K9me3 and H4Ac levels in stimulated DCs and 3T3s.
(F) Average levels of JmjD2d in stimulated DCs (Fi) between predicted enhancers and their nearest promoters, and (Fii) surrounding predicted enhancers.
(G) (Left) Distributions of JmjD2d levels around predicted enhancers in stimulated DCs. (Right) Fold change in H3K9me3 levels, upon LPS stimulation of DCs (top) or TNF-α stimulation of 3T3 fibroblasts (bottom), flanking enhancers associated with low (black) or high (red) levels of bound JmjD2d in DCs.
(H) Expression of *JmjD2d* mRNA (Hi) or protein (Hii) in LPS-stimulated wild-type and *JmjD2d*-knockdown DCs. mRNA levels are expressed relative to levels in unstimulated wild-type DCs. Protein levels were determined by flow cytometry and are expressed in arbitrary units; p65 protein levels in the same cell populations are shown for comparison.
(I) H3K9me3 levels at the *Mdc* and *Il12b* loci in wild-type and *JmjD2d*-knockdown DCs stimulated for 2 hr with LPS. The results presented in (A), (B), (H), and (I) are representative of three to five experiments. Statistical analysis and related experiments are shown in Figure S4; characterization of anti-JmjD2d antibodies is described in Figure S5.

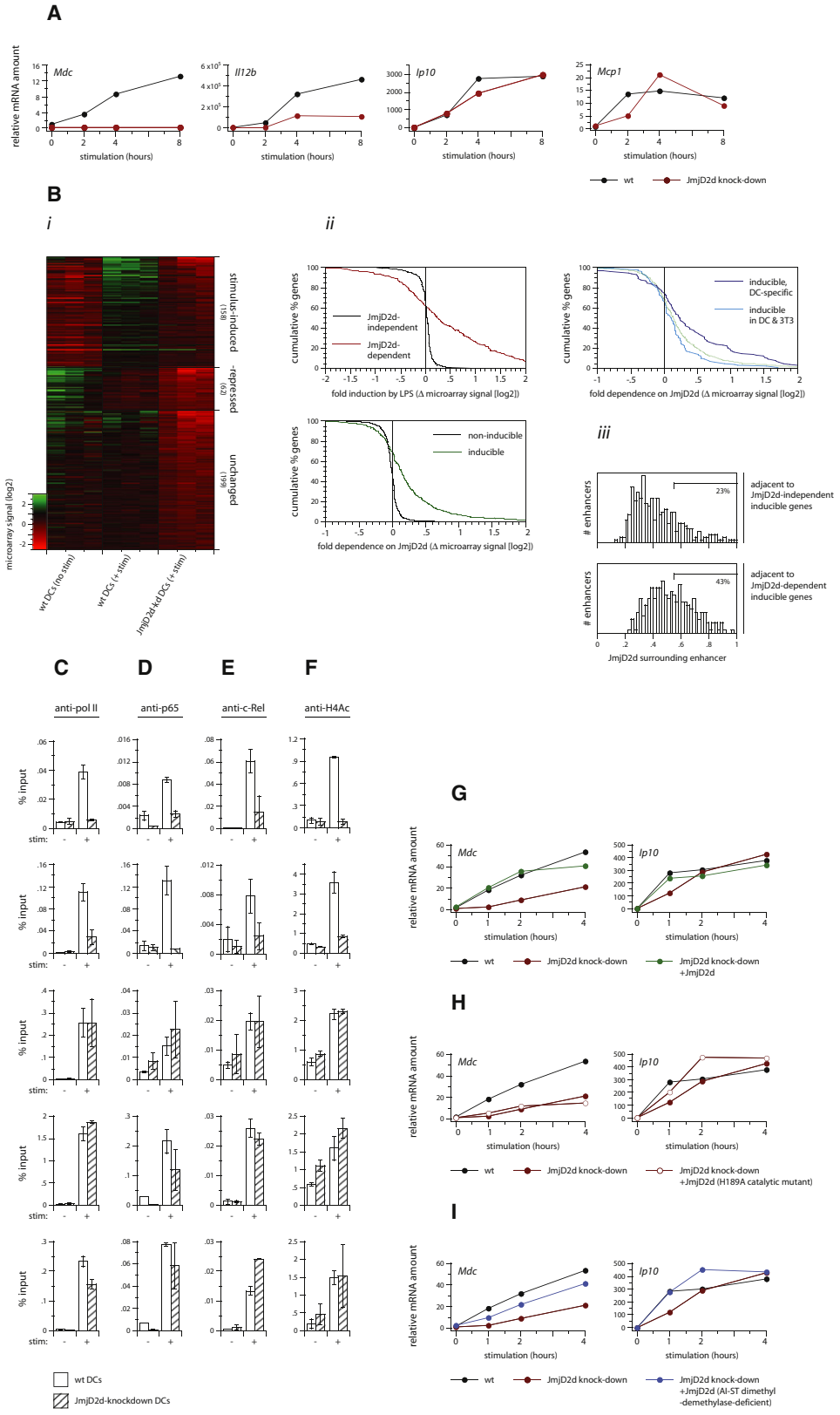
A
relative mRNA amount
Mdc
Il12b
Ip10
Mcp1
stimulation (hours)
wt
JmjD2d knock-down
B
i
ii
iii
stimulus-induced (158)
-repressed (92)
unchanged (1991)
microarray signal (log2)
wt DCs (no stim)
wt DCs (+stim)
JmjD2d-kd DCs (+stim)
cumulative % genes
JmjD2d-independent
JmjD2d-dependent
fold induction by LPS (Δ microarray signal [log2])
inducible, DC-specific
inducible in DC & 3T3
fold dependence on JmjD2d (Δ microarray signal [log2])
non-inducible
inducible
enhancers
23%
adjacent to JmjD2d-independent inducible genes
43%
adjacent to JmjD2d-dependent inducible genes
JmjD2d surrounding enhancer
C
D
E
F
anti-pol II
anti-p65
anti-c-Rel
anti-H4Ac
Mdc
Il12b
Ip10
Mip2
Il1b
% input
stim:
wt DCs
JmjD2d-knockdown DCs
G
H
I
JmjD2d knock-down +JmjD2d
JmjD2d knock-down +JmjD2d (H189A catalytic mutant)
JmjD2d knock-down +JmjD2d (AI-ST dimethyl -demethylase-deficient)

Enhancers are heterogeneous in their levels of associated JmjD2d in DCs (Figure 4G and Figures S4G–S4J), in line with their different levels of flanking H3K9me3. In stimulated DCs, around 7% of enhancers are bound by high levels of JmjD2d, and regions flanking most of these enhancers undergo a pronounced reduction in their relative levels of H3K9me3 trimethylation upon stimulation of DCs, but not fibroblasts (Figure 4G and Figure S4J)—indicating that JmjD2d binding at these regions is generally associated with enzymatic activity. The levels of JmjD2d were almost perfectly mirrored by those detected using the anti-JmjN domain antibody, indicating that enhancers which are not bound by Jmjd2d in DCs are also unlikely to be regulated by any of the other JmjD2 family members (Figure S4H).

To directly investigate the function of JmjD2d, we generated DCs from hematopoietic progenitor cells stably expressing shRNAs targeting the *JmjD2d* mRNA. *JmjD2d* mRNA levels in these knockdown DCs were reduced by more than 90%, and endogenous JmjD2d protein levels were reduced by at least 70% compared with control cells (either wild-type cells, or in cells expressing an irrelevant shRNA targeting *Gfp*; Figure 4H). We used two independent hairpins directed against nonoverlapping regions of the *JmjD2d* coding sequence to knock down *JmjD2d*, and both gave equivalent results (data not shown).

Prestimulation levels of H3K9me3 at and around the *Mdc* and *Il12b* enhancer and promoter regions were largely unchanged in *JmjD2d* knockdown DCs, with the knockdown cells still exhibiting the regions of higher-level H3K9me3 adjacent to and flanking both enhancers (Figure 4I). However, upon LPS stimulation, the pattern of H3K9 trimethylation at these loci was markedly altered: instead of the modest reductions in H3K9me3 levels that we saw in control cells, we observed the induction of significant H3K9 hypermethylation across the *Mdc* and *Il12b* loci in *JmjD2d*-knockdown DCs (Figure 4I). The overall behavior of H3K9 trimethylation in stimulated *JmjD2d*-knockdown DCs was reminiscent of that seen in stimulated 3T3 fibroblasts (Figures 2A and 2B): as in fibroblasts, high levels of H3K9me3 were induced at the *Mdc* and *Il12b* loci but were not observed at the promoter or enhancer regions of several other stimulus-responsive genes (Figure S4K). Likewise, the actual enhancers of *Mdc* and *Il12b* excluded the highest levels of H3K9 trimethylation, which instead appeared at adjacent genomic regions (Figure 4I). Also similarly to fibroblasts, the elevated surrounding levels of H3K9me3 did not preclude binding of transcription factors, since we found comparable recruitment of c-Rel and CEBP/β to the *Mdc* and *Il12b* enhancers in wild-type and *JmjD2d*-knockdown DCs (Figures S4L and S4M).

Together, these results indicate that binding of the demethylase JmjD2d is associated with the cell-type-specific regulation of H3K9me3 levels surrounding numerous enhancers in stimulated DCs. Intriguingly, although the reduction in H3K9me3 levels in stimulated wild-type DCs is fairly modest, the increase which results from JmjD2d deficiency is substantial, implying that a principal role of JmjD2d in myeloid cells may be to limit stimulus-induced H3K9 hypermethylation (Figure 2F), rather than to completely erase H3K9me3 levels. However, since H3K9me3 levels measured by ChIP represent the average across a large number of alleles, we cannot exclude the possibility that JmjD2d may also completely demethylate a subset of enhancers within a heterogeneous population.

H3K9me3 Demethylation by Jmjd2d Regulates Cell-Type-Specific Expression of *Mdc* and *Il12b*

The artificially high levels of H3K9me3 which are induced around the *Mdc* and *Il12b* enhancers in stimulated *JmjD2d* knockdown DCs (Figure 4I) allowed us to test whether this indeed has a functional downstream effect on gene activation at their endogenous target promoters, as suggested by the genome-wide distribution of H3K9me3 surrounding enhancers (Figures 2C–2F) and our experiments above using reporter plasmids (Figures 3B–3D).

We found that induction of both *Mdc* and *Il12b* mRNA expression was severely blocked in *JmjD2d* knockdown DCs (Figure 5A). Expression of many other control genes was unaffected, including inducible NF-κB target genes such as *Ip10* and *Mcp1*, at whose promoter/enhancer regions H3K9me3 levels remained low in the absence of JmjD2d (Figure 5A, Figures S6A and S4K). Microarray analysis indicated that the expression of around 400 genes was impaired by *JmjD2d* knockdown in DCs (Figure 5B). JmjD2d-dependent expression was highly enriched among stimulus-inducible genes, and even further among those showing specific expression in DCs, with the majority being positively regulated by JmjD2d (Figure 5Bii). Enhancers adjacent to stimulus-induced JmjD2d-dependent genes were strongly enriched for local JmjD2d binding by ChIP (Figure 5Biii), suggesting that regulation is direct (see also Figure S6B and legend). Nonetheless, a fraction of enhancers with associated JmjD2d binding are also found adjacent to genes unaffected by *JmjD2d* knockdown, suggesting either that JmjD2d binding at these locations may be nonfunctional, or that these

Figure 5. H3K9me3 Demethylation by JmjD2d Is Required for Expression of *Mdc* and *Il12b* in DCs

(A) Expression of *Mdc*, *Il12b*, *Ip10*, and *Mcp1* mRNA in wild-type and *JmjD2d*-knockdown DCs stimulated with LPS, relative to levels in unstimulated wild-type cells.

(B) (Bi) Relative expression levels of all genes showing impaired expression in *JmjD2d*-knockdown DCs, grouped according to their expression profiles in wild-type DCs. (Bii) Cumulative percentages of (top left) JmjD2d-dependent or -independent genes whose expression is induced upon LPS stimulation by greater than the indicated amount; (bottom left) noninduced or LPS-induced genes, or (top right) DC-specific or nonspecific LPS-induced genes, whose expression level is reduced in *JmjD2d* knockdown DCs by greater than the indicated amount. (Biii) Distributions of JmjD2d levels in stimulated DCs, around predicted enhancers adjacent to promoters of inducible *JmjD2d*-independent (top) or -dependent (bottom) genes.

(C–F) ChIP of promoter regions, in wild-type and *JmjD2d*-knockdown DCs, using antibodies against RNA polymerase II (C), NF-κB p65 (D), NF-κB c-Rel (E), and acetylated histone H4 (F), before and 2 hr after stimulation with LPS.

(G–I) *Mdc* and *Ip10* mRNA expression in wild-type and *JmjD2d*-knockdown DCs, and in *JmjD2d*-knockdown DCs retrovirally expressing JmjD2d (G), a catalytic null mutant of JmjD2d (H), or a dimethyl demethylation-deficient mutant of JmjD2d (I). Error bars indicate SEMs of replicate quantitations. The results presented in (A) and (C)–(I) are representative of three to six experiments. Statistical analysis and related experiments are described in Figure S6.

enhancers are dispensable for gene expression in this cellular context.

The lack of *Mdc* and *Il12b* mRNA expression in *JmjD2d*-knockdown DCs was mirrored by impaired RNA polymerase II recruitment to their promoter regions (Figure 5C). To explore the reason for this, we next examined promoter binding by NF-κB family transcription factors, which are essential for the activition of both of these promoters (Sanjabi et al., 2000; van Essen et al., 2010). We found that stimulus-induced recruitment of two transcriptionally active subunits of the NF-κB family, p65 and c-Rel, was significantly reduced at the promters of *Mdc* and *Il12b*, but not at those of other control NF-κB target genes (Figures 5D and 5E). Previous studies have shown that promoter binding by NF-κB can be controlled by prior marking of promoters by histone H4 hyperacetylation (Saccani et al., 2001), and that stable binding to the *Mdc* and *Il12b* promoters in particular is further regulated by Aof1-dependent removal of H3K9 dimethylation (van Essen et al., 2010). We therefore examined the behavior of both of these histone modifications at the *Mdc* and *Il12b* promoters in *JmjD2d* knockdown DCs. We found that, at these promoters, stimulus-induced H4 hyperacetylation was strongly reduced, in contrast to the high levels observed at the promoters of control genes (Figure 5F). Moreover, stimulus-induced demethylation of H3K9me2 at the *Mdc* and *Il12b* promoters was also prevented in *JmjD2d* knockdown DCs (Figure S6D). Thus, knockdown of *JmjD2d* in stimulated DCs results in impaired changes to histone modifications, transcription factor binding, RNA polymerase II recruitment, and mRNA transcription at the *Mdc* and *Il12b* promoters.

We next tested whether the catalytic activity of JmjD2d was responsible for the effects we had observed on gene activity. Reconstitution of *JmjD2d*-knockdown cells with a retrovirally expressed, shRNA-resistant form of JmjD2d restored *Mdc* mRNA expression to wild-type levels (Figure 5G). In contrast, a catalytically inactive mutant of JmjD2d bearing a point mutation predicted to prevent Fe_{II} binding (H189A; based on Whetstine et al., 2006) was completely unable to restore *Mdc* mRNA expression (Figure 5H and Figure S6E). Wild-type JmjD2d is able to demethylate trimethyl and dimethyl H3K9 (Chen et al., 2006; Whetstine et al., 2006) and has also been reported to have low activity against monomethyl H3K9 (Couture et al., 2007). To discriminate which of these catalytic activities are involved in its regulation of gene expression, we engineered a mutant form of JmjD2d (A289S/I290T) predicted to mimic the methyl state specificity of JmjD2a, which preferentially demethylates trimethylated lysine and exhibits only very weak or no activity against the dimethyl or monomethyl states (Figure 5I and Figure S6E; Chen et al., 2006; Whetstine et al., 2006). This mutant was also able to substantially rescue *Mdc* expression in stimulated *JmjD2d* knockdown DCs, although the *Mdc* mRNA levels were lower than those achieved using wild-type JmjD2d (Figures 5G and 5I). These data together argue that the cell-type-specific control of transcriptional activity at the *Mdc*, *Il12b*, and other promoters by JmjD2d is primarily or entirely mediated through its regulation of trimethylated H3K9, which is principally located at distal regions harboring their enhancers.

Since stimulated 3T3 fibroblasts, which do not naturally express JmjD2d (Figure 4A), exhibit high levels of H3K9me3 flanking the *Mdc* and *Il12b* enhancers (Figures 2A and 2B), we explored whether ectopic expression of JmjD2d alone would be able to reduce these levels, and whether this would be sufficient to activate transcription from the *Mdc* and *Il12b* promoters.

We transduced fibroblasts with a retrovirus driving expression of JmjD2d, and examined H3K9me3 levels at the *Mdc* and *Il12b* loci after stimulation with TNF-α. Ectopic JmjD2d expression dramatically reduced the levels of H3K9 trimethylation induced around both enhancers compared to untransduced cells (Figure 6A). As expected, this required the demethylase activity of JmjD2d, as no effect was observed when using the catalytically inactive mutant (data not shown). The reduction in H3K9me3 levels around the *Mdc* and *Il12b* enhancers in JmjD2d-expressing fibroblasts was accompanied by the acquisition of stimulus-dependent transcriptional activation of both of these genes (Figure 6B). Ectopic JmjD2d expression did not significantly alter the stimulus-induced expression of other control genes (such as *Ip10*), and it was unable to induce expression of the DC-specific *Il1b* gene (Figure 6B), whose expression in DCs is not dependent on JmjD2d (Figures S1B and S6A). LPS stimulation, which is generally a poor inducer of gene activation in fibroblasts and is insufficient to trigger expression of the control *Ip10* gene, was nevertheless adequate to trigger *Mdc* and *Il12b* expression in JmjD2d-expressing fibrobasts (Figure 6B). Interestingly, although forced expression of JmjD2d alone was sufficient to allow expression of the normally myeloid-specific *Mdc* and *Il12b* genes in transduced fibroblasts, the levels of mRNA produced were still much lower than those seen in stimulated DCs, indicating that full activation of these genes may involve additional myeloid-specific regulatory mechanisms (for instance, other candidate enhancers detected at the *Il12b* locus; Figure 1E).

H3K9 Trimethylation Controls Broadly Functional Enhancers Associated with Cell-Type-Specific Gene Expression

The experiments described so far indicate that despite the cell-type-specific expression of *Mdc* and *Il12b*, both genes are associated with enhancers which are broadly functional when assayed in isolation. At these genes, and many others throughout the genome, cell-type-specific control of expression is linked to the presence of high levels of H3K9 trimethylation at regions surrounding distal enhancers, and we experimentally found that this is able to repress the activities of the *Mdc* and *Il12b* enhancers in both episomal and genomically integrated contexts. Moreover, artificial perturbation of the H3K9me3 levels around the endogenous *Mdc* and *Il12b* enhancers, by knockdown or ectopic expression of the normally myeloid-specific demethylase JmjD2d, was able to switch the cell-type specificity of gene activation. These data reveal that the regulation of local H3K9me3 levels represents a key step in controlling the cell-type-specific activities of the *Mdc* and *Il12b* enhancers.

The presence of high levels of H3K9me3 in regions flanking a substantial fraction of predicted enhancers in cells where the adjacent genes are inactive (Figure 2E and Figure S2G) strongly suggests that this is a common mechanism for regulating their

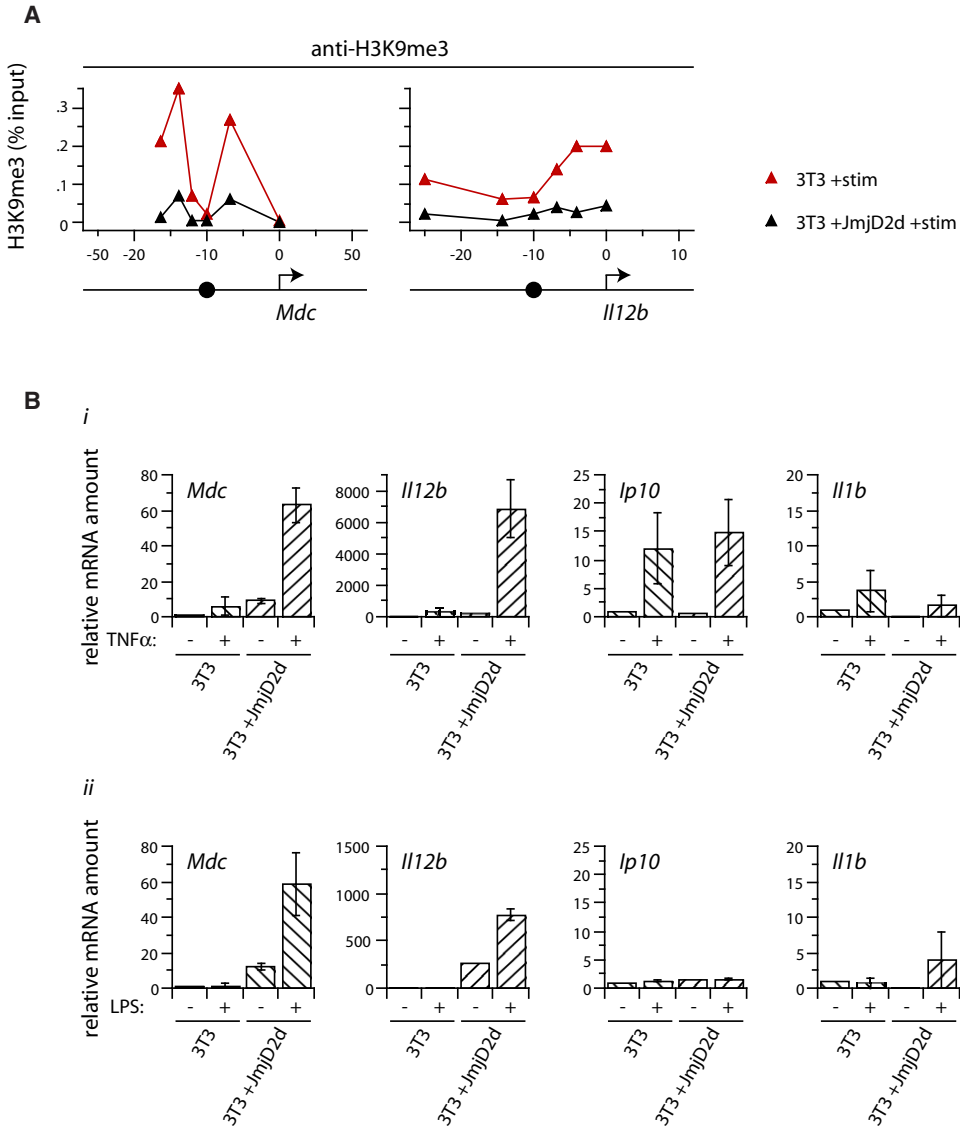

Figure 6. Ectopic Expression of JmjD2d in 3T3 Fibroblasts Induces H3K9me3 Demethylation and Expression of *Mdc* and *Il12b*

(A) H3K9me3 at the *Mdc* and *Il12b* loci, and (B) mRNA expression in wild-type 3T3 fibroblasts and in fibroblasts ectopically expressing JmjD2d, after stimulation for 2 hr with (Ai) TNF-α or (Aii) LPS. mRNA levels are relative to those in unstimulated wild-type 3T3s. Error bars indicate SEMs of replicate quantitations. The results presented here are representative of two to three experiments. Statistical analysis is described in the legend to Figure S6.

cell-type-specific activity. If this is the case, it follows that such enhancers should exhibit a *non*-cell-type-specific function if assayed when removed from such regulation. To test this, we began by using publically available data sets to identify enhancers whose levels of flanking H3K9me3 correlated with the differential expression of their adjacent genes in three human hematopoietic cell types (CD133+ progenitor cells, CD36+ erythroblasts, and CD4+ T cells). We reasoned that the common origin of these related cell types should increase the likelihood that any observed differences in chromatin modifications would result from active processes regulating gene expression, rather than simply recalling past events in their developmental histories. We selected a representative subset of these enhancers (hereafter termed "H3K9me3-associated") and cloned their mouse counterparts into reporter plasmids. We then measured their function when transfected into a panel of different mouse cell types. We also examined a group of control enhancers, which were linked to genes with cell-type-specific expression, but which did not show evidence of regulation by H3K9me3 and were therefore expected to display an inherently cell-type-specific function (as has been described for other enhancers; Ghisletti et al., 2010; Heintzman and Ren, 2009). Using 12 different cell lines derived from diverse sources (B and T lymphocytes, gut epithelium, erythroblasts, fibroblasts, macrophages, mammary epithelium, myoblasts, neuroblasts, salivary gland epithelium, thymic stroma, and trophoblast stem cells), none of

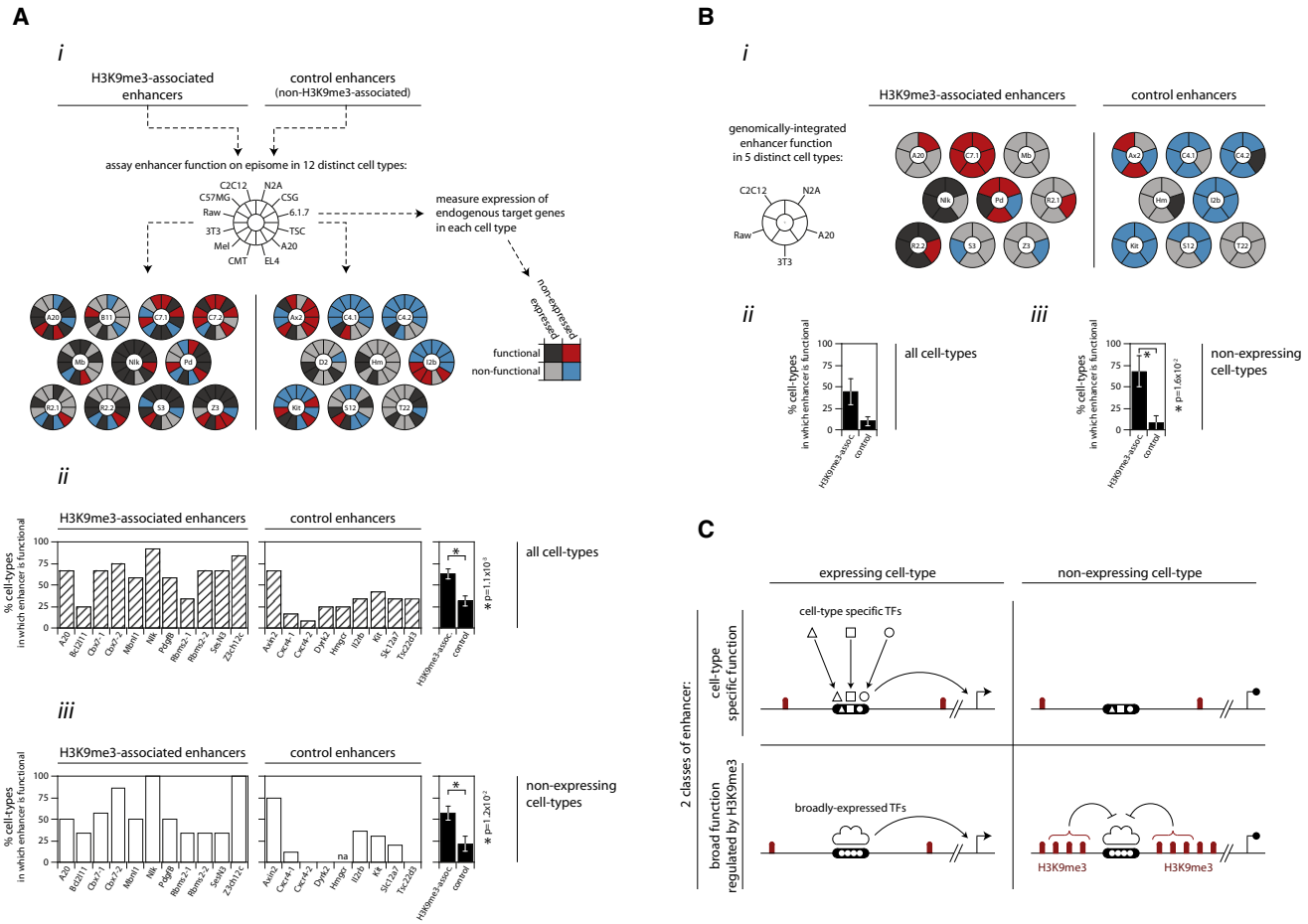

Figure 7. H3K9 Trimethylation Controls Broadly Functional Enhancers Associated with Cell-Type-Specific Gene Expression

(A) Functionality of cloned enhancer sequences in episomal reporter assays; (Ai) individually for all cel types tested, indicated by color in the corresponding cake slice, (Aii) as a percentage of all cell types tested, and (Aiii) as a percentage of only those cell types in which the putative target gene of each enhancer is nonexpressed. The mean percentage for each group of enhancers is shown in the right panels.

(B) Functionality of cloned enhancer sequences in stable, genomically integrated reporter assays, depicted as in (A). Error bars represent SEMs.

(C) Schematic illustration of the mechanisms used by distinct classes of enhancers to achieve cell-type-specific activity. The results presented here are representative of four to five experiments. Statistical analysis and related experiments are described in Figure S7.

the enhancers tested were ubiquitously functional in every cell type. However, there were significant differences in the number of cell types in which enhancers from each group were functional: H3K9me3-associated enhancers tended to be broadly functional, displaying function in a mean of 63% of tested cell types. In contrast, the control (non-H3K9me3-associated) enhancers showed a significantly more restricted function, on average in only 31% of cell types (Figure 7A).

The model in which H3K9me3 regulates cell-type-specific enhancer activity not only predicts that H3K9me3-associated enhancers should be broadly functional, but in particular predicts that this class of enhancers should often be functional, when tested on a plasmid, in cell types which do not express their target genes. To test this, we began by assessing whether the putative target genes of each enhancer (based on simple proximity in the genome) were expressed in each of the cell lines, by measuring their mRNA expression levels. The genes associated with each group of enhancers were active in a similar proportion of cell lines (Figure S7A), irrespective of the cutoff levels of mRNA used to discriminate expressed from non-expressed genes. We then reanalyzed the function of the two groups of enhancers, considering only cell types in which their putative target genes were nonexpressed. H3K9me3-associated enhancers were still highly functional in 57% of non-expressing cell types (Figure 7Aiii), similar to their behavior when considering all cell types (Figure 7Aii). This is consistent with the idea that these enhancer sequences are capable of driving target gene expression, but that the local chromatin environment of their endogenous counterparts is responsible for their cell-type-specific repression (although note that we have not explicitly measured H3K9me3 levels surrounding every enhancer in all tested cell types). The function of the control enhancers matched more closely the expression patterns of their endogenous target genes, with significantly fewer (22%; $p = 1.2 \times 10^{-2}$)

nonexpressing cell lines still exhibiting enhancer function, corroborating the notion that in these cases cell-type-specific gene expression generally matches the cell-type-specific function of their enhancers.

We also assayed the function of enhancers from each group using genomically integrated reporter constructs, which more closely recapitulate the chromatin environment in which enhancers must normally function. This setup restricted the function of many of the tested enhancer sequences, such that all except one of the control enhancers lost measurable function in nonexpressing cell types (Figure 7B). Importantly, though, the H3K9me3-associated enhancers were often still functional in multiple cell types, including those which do not express their endogenous target genes (Figures 7Bii and 7Biii; $p = 1.6 \times 10^{-2}$).

Together, these results indicate that the association of flanking H3K9me3 levels with differential target gene expression in related cell types is characteristic of enhancers which, when assayed in isolation, exhibit a broad, *non*-cell-type-specific function. In contrast, enhancers which regulate differential target gene expression, but without carrying high levels of flanking H3K9me3, generally display an inherent cell-type specificity, and, accordingly, their function is only measurable in cell types in which their endogenous target genes are active.

These data imply that the mechanistic link between H3K9 trimethylation and the repression of enhancer activity, which we characterized above for the *Mdc* and *Il12b* enhancers (Figures 3B–3D, Figure 4I, Figure 5A, and Figure 6), is widely applicable to other broadly functional enhancers. To confirm this, we tested the ability of targeted Gal4DBD-Suv39h1 to repress each of those H3K9me3-associated enhancers which were functional in 3T3 fibroblasts, using the same experimental setup as used in Figure 3B. As predicted, the activities of all tested enhancers were inhibited by Gal4DBD-Suv39h1 in a methyltransferase activity-dependent fashion (Figure S7D). Thus, the presence of local high-level H3K9me3 not only correlates with the cell-type-specific repression of many enhancers in their natural genomic context, but it is also sufficient for their repression when assayed on an episomal plasmid.

Finally, we wished to test whether we could predict additional genes whose endogenous expression levels would change upon artificial perturbation of H3K9me3 levels, using only our knowledge of their enhancer function in reporter assays and its association with H3K9me3. Our assayed subset of H3K9me3-associated enhancers contains three which are located adjacent to genes which are not expressed in 3T3 fibroblasts: two lie close together upstream of the *Cbx7* gene, and one lies upstream of the neighboring *PdgfB* gene. Each of these enhancer sequences is functional in 3T3 fibroblasts when assayed using a transfected reporter plasmid, suggesting that the activities of their endogenous counterparts are repressed by high levels of H3K9me3 at their native genomic loci. We therefore explored the behavior of these genes, in fibroblasts ectopically overexpressing the H3K9me3 demethylase JmjD2d. JmjD2d overexpression caused a substantial reduction in the H3K9me3 levels flanking each of these enhancers, compared to wild-type cells, and resulted in significant transcriptional activation of both genes (Figure S7E). Thus, H3K9me3 levels appear to regulate the activities of these enhancers in their native genomic contexts.

DISCUSSION

We have shown that regions of high-level H3K9 trimethylation are able to act in *cis* to repress the activities of enhancers upstream of the *Mdc* and *Il12b* genes, and also of numerous other enhancers found throughout the genome. This is in accord with observations made by Zhang et al. (2008) of the *reaper/hid* enhancer in *Drosophila*. When assayed outside their natural genomic context, many such enhancers are able to drive gene expression in cell types where their endogenous target genes are inactive. This suggests that regulation by regions of high-level H3K9me3 is a widely used mechanism to impart cell-type-specific activity onto otherwise broadly functional enhancers (as schematically depicted in Figure 7C).

Although H3K9me3 is well known as a principal component of heterochromatin, its role in euchromatic regions has remained less clear. H3K9me3-rich regions have been described to occur in contiguous blocks, covering around 16% of the genome in fibroblasts, and these are underrepresented for inclusion of promoter regions (Hawkins et al., 2010). Instead, this mark is widely present in intergenic regions, and spreading of H3K9me3 into these regions has been associated with irreversible gene silencing during differentiation (Su et al., 2004). H3K9me3 is often located at and around repetitive sequences (Barski et al., 2007), and Mikkelsen et al. (2007) noted that its spreading implied a potential to regulate local unique sequences. We find that genomic regions containing high-level H3K9me3 act to repress adjacent enhancer activity, and that cell-type-specific differences in the distributions of high-level H3K9me3 around enhancers correlate with target gene expression. Based on this, we propose that the widespread presence of intergenic H3K9me3 plays an important and general role regulating enhancer activity, to control the cell-type specificity of gene expression.

EXPERIMENTAL PROCEDURES

Cell Culture

Progenitor cells from mouse bone marrow were differentiated in vitro into DCs for 8–10 days in GM-CSF. DCs were stimulated with 100 $ngml^{-1}$ LPS or 10 $ngml^{-1}$ TNF-α; 3T3 fibroblasts were stimulated with 10 μgml^{-1} LPS or 10 $ngml^{-1}$ TNF-α. Retroviruses were produced using Ecotropic-Phoenix packaging cells; Raw 264.7 macrophages and 3T3 fibroblasts were transfected with plasmids using lipofectamine. See the Supplemental Experimental Procedures for additional details.

Plasmids

Promoters and enhancers were assayed episomally using pGL3-GFP (a variant of pGL3 [Promega] in which the luciferase coding sequence is replaced with that of GFP); promoter fragments were inserted immediately upstream of the GFP CDS, and enhancer fragments were inserted downstream of the polyadenylation signal following GFP. Enhancers were assayed after genomic integration using the self-inactivating lentiviral vector pSIN-minTK-GFP, with enhancer fragments inserted immediately upstream of the minimal TK promoter. Endogenous JmjD2d was stably knocked down in DCs using shRNAs directed against the coding sequence, and ectopic expression of JmjD2d was driven in 3T3 fibroblasts from the retroviral vector pMY-ires-Tomato. See the Supplemental Experimental Procedures for full details of plasmids used.

Antibodies

Antibodies used are listed in the Supplemental Experimental Procedures.

ChIP and RT-PCR

ChIP was performed as described (Olszak et al., 2011; Saccani and Natoli, 2002). All PCR and RT-PCR were performed using quantitative analysis with gene-specific fluorescent probes. Primer sequences are available on request. mRNA levels are normalized with respect to *Tbp* and expressed relative to unstimulated, wild-type cells.

Analysis of Genome-wide Data Sets

Candidate enhancers were identified as peaks of H3K4me1 identified using MACS14 and paired with their closest annotated promoters. Promoter activity was determined using microarray expression data for the corresponding transcript. Distributions of tag densities for H3K9me3, JmjD2d, and JmjD2 family protiens, which do not fall into discrete peaks, were normalized by calculating the ratio to input tags in 2 kb bins every 200 bp. Enhancers used for functional analysis were selected from among those predicted by Heintzman et al. (2009), according to their surrounding H3K9me3 and gene expression levels in data sets from human CD4 T cells, CD36 erythroblasts, and CD133 HPCs (Barski et al., 2007; Cui et al., 2009), and the corresponding mouse genomic subregions carrying enhancer function were identified using episomal enhancer assays. See the Supplemental Experimental Procedures for additional details.

Statistical Analysis

Statistical differences between experimental groups were analyzed using two-tailed Student's t tests. p values associated with distributions of gene expression levels or ChIP-Seq tag densities were determined using chi-squared tests on 2 × 2 tables in which genes or enhancers were separated into groups according to a fixed threshold.

ACCESSION NUMBERS

Data described in this study have been deposited at the National Center for Biotechnology Information (NCBI) Gene Expression Omnibus (GEO) database (http://www.ncbi.nlm.nih.gov/geo/) with accession number GSE32381.

SUPPLEMENTAL INFORMATION

Supplemental Information includes seven figures, one table, Supplemental Experimental Procedures, and Supplemental References and can be found with this article online at doi:10.1016/j.molcel.2012.05.011.

ACKNOWLEDGMENTS

We are grateful to I. de la Rosa Velázquez and T. Manke for advice and expert assistance with ChIP sequencing, H. Kimura for providing anti-H3K9me3 and anti-H3K4me1 monoclonal antibodies, J. Wysocka for providing the retroviral vector used for enhancer assays, and R. Grosschedl for critical reading of the manuscript. This work was supported by grants from the European Union and the German Research Council.

Received: September 2, 2011
Revised: April 15, 2012
Accepted: May 8, 2012
Published online: May 24, 2012

REFERENCES

Barski, A., Cuddapah, S., Cui, K., Roh, T.Y., Schones, D.E., Wang, Z., Wei, G., Chepelev, I., and Zhao, K. (2007). High-resolution profiling of histone methylations in the human genome. Cell *129*, 823–837.

Borok, M.J., Tran, D.A., Ho, M.C., and Drewell, R.A. (2010). Dissecting the regulatory switches of development: lessons from enhancer evolution in Drosophila. Development *137*, 5–13.

Bulger, M., and Groudine, M. (2011). Functional and mechanistic diversity of distal transcription enhancers. Cell *144*, 327–339.

Chen, Z., Zang, J., Whetstine, J., Hong, X., Davrazou, F., Kutateladze, T.G., Simpson, M., Mao, Q., Pan, C.H., Dai, S., et al. (2006). Structural insights into histone demethylation by JMJD2 family members. Cell *125*, 691–702.

Couture, J.F., Collazo, E., Ortiz-Tello, P.A., Brunzelle, J.S., and Trievel, R.C. (2007). Specificity and mechanism of JMJD2A, a trimethyllysine-specific histone demethylase. Nat. Struct. Mol. Biol. *14*, 689–695.

Creyghton, M.P., Cheng, A.W., Welstead, G.G., Kooistra, T., Carey, B.W., Steine, E.J., Hanna, J., Lodato, M.A., Frampton, G.M., Sharp, P.A., et al. (2010). Histone H3K27ac separates active from poised enhancers and predicts developmental state. Proc. Natl. Acad. Sci. USA *107*, 21931–21936.

Cui, K., Zang, C., Roh, T.Y., Schones, D.E., Childs, R.W., Peng, W., and Zhao, K. (2009). Chromatin signatures in multipotent human hematopoietic stem cells indicate the fate of bivalent genes during differentiation. Cell Stem Cell *4*, 80–93.

Ghadially, H., Ross, X.L., Kerst, C., Dong, J., Reske-Kunz, A.B., and Ross, R. (2005). Differential regulation of CCL22 gene expression in murine dendritic cells and B cells. J. Immunol. *174*, 5620–5629.

Ghisletti, S., Barozzi, I., Mietton, F., Polletti, S., De Santa, F., Venturini, E., Gregory, L., Lonie, L., Chew, A., Wei, C.L., et al. (2010). Identification and characterization of enhancers controlling the inflammatory gene expression program in macrophages. Immunity *32*, 317–328.

Hawkins, R.D., Hon, G.C., Lee, L.K., Ngo, Q., Lister, R., Pelizzola, M., Edsall, L.E., Kuan, S., Luu, Y., Klugman, S., et al. (2010). Distinct epigenomic landscapes of pluripotent and lineage-committed human cells. Cell Stem Cell *6*, 479–491.

Heintzman, N.D., and Ren, B. (2009). Finding distal regulatory elements in the human genome. Curr. Opin. Genet. Dev. *19*, 541–549.

Heintzman, N.D., Hon, G.C., Hawkins, R.D., Kheradpour, P., Stark, A., Harp, L.F., Ye, Z., Lee, L.K., Stuart, R.K., Ching, C.W., et al. (2009). Histone modifications at human enhancers reflect global cell-type-specific gene expression. Nature *459*, 108–112.

Hoffmann, A., and Baltimore, D. (2006). Circuitry of nuclear factor kappaB signaling. Immunol. Rev. *210*, 171–186.

Horvai, A., Palinski, W., Wu, H., Moulton, K.S., Kalla, K., and Glass, C.K. (1995). Scavenger receptor A gene regulatory elements target gene expression to macrophages and to foam cells of atherosclerotic lesions. Proc. Natl. Acad. Sci. USA *92*, 5391–5395.

Hublitz, P., Albert, M., and Peters, A.H. (2009). Mechanisms of transcriptional repression by histone lysine methylation. Int. J. Dev. Biol. *53*, 335–354.

Kouzarides, T. (2007). Chromatin modifications and their function. Cell *128*, 693–705.

Levine, M., and Tjian, R. (2003). Transcription regulation and animal diversity. Nature *424*, 147–151.

Mikkelsen, T.S., Ku, M., Jaffe, D.B., Issac, B., Lieberman, E., Giannoukos, G., Alvarez, P., Brockman, W., Kim, T.K., Koche, R.P., et al. (2007). Genome-wide maps of chromatin state in pluripotent and lineage-committed cells. Nature *448*, 553–560.

Murphy, T.L., Cleveland, M.G., Kulesza, P., Magram, J., and Murphy, K.M. (1995). Regulation of interleukin 12 p40 expression through an NF-kappa B half-site. Mol. Cell. Biol. *15*, 5258–5267.

Natoli, G., and De Santa, F. (2006). Shaping alternative NF-kappaB-dependent gene expression programs: new clues to specificity. Cell Death Differ. *13*, 693–696.

Nottke, A., Colaiacovo, M.P., and Shi, Y. (2009). Developmental roles of the histone lysine demethylases. Development *136*, 879–889.

Olszak, A.M., van Essen, D., Pereira, A.J., Diehl, S., Manke, T., Maiato, H., Saccani, S., and Heun, P. (2011). Heterochromatin boundaries are hotspots for de novo kinetochore formation. Nat. Cell Biol. *13*, 799–808.

Plevy, S.E., Gemberling, J.H., Hsu, S., Dorner, A.J., and Smale, S.T. (1997). Multiple control elements mediate activation of the murine and human

interleukin 12 p40 promoters: evidence of functional synergy between C/EBP and Rel proteins. Mol. Cell. Biol. *17*, 4572–4588.

Rada-Iglesias, A., Bajpai, R., Swigut, T., Brugmann, S.A., Flynn, R.A., and Wysocka, J. (2011). A unique chromatin signature uncovers early developmental enhancers in humans. Nature *470*, 279–283.

Saccani, S., and Natoli, G. (2002). Dynamic changes in histone H3 Lys 9 methylation occurring at tightly regulated inducible inflammatory genes. Genes Dev. *16*, 2219–2224.

Saccani, S., Pantano, S., and Natoli, G. (2001). Two waves of nuclear factor kappaB recruitment to target promoters. J. Exp. Med. *193*, 1351–1359.

Sanjabi, S., Hoffmann, A., Liou, H.C., Baltimore, D., and Smale, S.T. (2000). Selective requirement for c-Rel during IL-12 P40 gene induction in macrophages. Proc. Natl. Acad. Sci. USA *97*, 12705–12710.

Sen, R., and Smale, S.T. (2010). Selectivity of the NF-{kappa}B response. Cold Spring Harb. Perspect. Biol. *2*, a000257. 10.1101/cshperspect.a000257.

Smale, S.T. (2010). Selective transcription in response to an inflammatory stimulus. Cell *140*, 833–844.

Snowden, A.W., Gregory, P.D., Case, C.C., and Pabo, C.O. (2002). Gene-specific targeting of H3K9 methylation is sufficient for initiating repression in vivo. Curr. Biol. *12*, 2159–2166.

Su, R.C., Brown, K.E., Saaber, S., Fisher, A.G., Merkenschlager, M., and Smale, S.T. (2004). Dynamic assembly of silent chromatin during thymocyte maturation. Nat. Genet. *36*, 502–506.

van Essen, D., Zhu, Y., and Saccani, S. (2010). A feed-forward circuit controlling inducible NF-kappaB target gene activation by promoter histone demethylation. Mol. Cell *39*, 750–760.

Visel, A., Rubin, E.M., and Pennacchio, L.A. (2009). Genomic views of distant-acting enhancers. Nature *461*, 199–205.

Wang, Z., Zang, C., Cui, K., Schones, D.E., Barski, A., Peng, W., and Zhao, K. (2009). Genome-wide mapping of HATs and HDACs reveals distinct functions in active and inactive genes. Cell *138*, 1019–1031.

Whetstine, J.R., Nottke, A., Lan, F., Huarte, M., Smolikov, S., Chen, Z., Spooner, E., Li, E., Zhang, G., Colaiacovo, M., et al. (2006). Reversal of histone lysine trimethylation by the JMJD2 family of histone demethylases. Cell *125*, 467–481.

Zhang, Y., Lin, N., Carroll, P.M., Chan, G., Guan, B., Xiao, H., Yao, B., Wu, S.S., and Zhou, L. (2008). Epigenetic blocking of an enhancer region controls irradiation-induced proapoptotic gene expression in Drosophila embryos. Dev. Cell *14*, 481–493.

Zhou, L., Nazarian, A.A., Xu, J., Tantin, D., Corcoran, L.M., and Smale, S.T. (2007). An inducible enhancer required for Il12b promoter activity in an insulated chromatin environment. Mol. Cell. Biol. *27*, 2698–2712.